

# Training Algorithm Matters for the Performance of Neural Network Potential

Yunqi Shao,<sup>†</sup> Florian M. Dietrich,<sup>†</sup> Carl Nettelblad,<sup>‡</sup> and Chao Zhang<sup>\*,†</sup>

<sup>†</sup>*Department of Chemistry-Ångström Laboratory, Uppsala University, Lägerhyddsvägen 1, BOX 538, 75121, Uppsala, Sweden*

<sup>‡</sup>*Division of Scientific Computing, Department of Information Technology, Uppsala University, Lägerhyddsvägen 2, BOX 337, 75105, Uppsala, Sweden*

E-mail: chao.zhang@kemi.uu.se

## Abstract

One hidden yet important issue for developing neural network potentials (NNPs) is the choice of training algorithm. Here we compare the performance of two popular training algorithms, the adaptive moment estimation algorithm (Adam) and the extended Kalman filter algorithm (EKF), using the Behler-Parrinello neural network (BPNN) and two publicly accessible datasets of liquid water. It is found that NNPs trained with EKF are more transferable and less sensitive to the value of the learning rate, as compared to Adam. In both cases, error metrics of the test set do not always serve as a good indicator for the actual performance of NNPs. Instead, we show that their performance correlates well with a Fisher information based similarity measure.

## Introduction

Neural network potentials (NNP) are one category of machine learning potentials<sup>1–4</sup> which approximate potential energy surfaces (PES) and allow for large-scale simulations with the accuracy of reference electronic structure calculations but at only a fraction of the computational cost.<sup>5</sup>

One prominent architecture of NNPs are Behler-Parrinello neural networks<sup>6</sup> which introduced the idea of partitioning the total

potential energy of the system into effective atomic contributions. BPNNs have been applied to a wide range of molecules and materials<sup>7–12</sup> Despite these successes, the BPNN architecture relies on the selection of a set of symmetry functions before the training in order to describe the local chemical environments. On the contrary, features in deep-learning<sup>13</sup> are automatically learned via hierarchical filters, rather than handcrafted. In particular, graph convolution neural networks (GCNN), which consider the atoms as nodes and the pairwise interactions as weighted edges in the graph, have emerged as a new type of architectures in constructing NNPs for both molecules and materials.<sup>14–16</sup>

Innovations regarding new architectures certainly drive the improvement of the performance of NNPs. However, one hidden and less discussed issue is the impact of training algorithms on the construction of NNPs. As a matter of fact, earlier implementations of BPNNs<sup>17–21</sup> used either the Limited-memory Broyden-Fletcher-Goldfarb-Shanno algorithm (LBFGS)<sup>22</sup> or the Extended Kalman Filter algorithm (EKF)<sup>23</sup> as the default optimizer, while recent implementations of GCNN architectures<sup>14–16,24</sup> almost exclusively chose the adaptive moment estimation algorithm (Adam)<sup>25</sup> instead. This contrast is, partly, due to the convenience that efficient implementations of Adam are available on popular frameworks such

as TensorFlow<sup>26</sup> and PyTorch.<sup>27</sup> Nevertheless, the practical equivalence among optimization algorithms for training NNPs is assumed rather than verified.

In this work, by implementing EKF in TensorFlow, we systematically compare the performance of two popular training algorithms, Adam and EKF, using BPNNs and two publicly accessible datasets of liquid water. We find that training algorithms have a non-trivial impact on the performance of NNPs, both in terms of extrapolation and interpolation. Before showing these results, we will outline the details of our comparative study, including the training algorithms, datasets, and molecular dynamics simulations used for the density prediction, as described in the next section.

## Methods

### Algorithms

In the following, we first introduce the common notations used for the optimization algorithm, and then briefly state the Adam and EKF algorithms compared within this work.

---

**Algorithm 1:** The Adam optimizer, where  $\eta$  is the learning rate,  $\epsilon$  is a small number,  $\beta_1$ ,  $\beta_2$  are the exponential moving average factors,  $\mathbf{m}$ ,  $\mathbf{v}$  are the first and second moment estimates and  $\hat{\mathbf{m}}(t)$  and  $\hat{\mathbf{v}}(t)$  are the bias-corrected moment estimates.

---

```

init:  $t = 0$ ,  $\mathbf{m}(0) = 0$ ,  $\mathbf{v}(0) = 0$ 
while not converged do
     $t = t + 1$ ;
     $\mathbf{g}(t) = \nabla_{\mathbf{w}} L(t)$ ;
     $\mathbf{m}(t) = \beta_1 \cdot \mathbf{m}(t-1) + (1 - \beta_1) \cdot \mathbf{g}(t)$ ;
     $\mathbf{v}(t) = \beta_2 \cdot \mathbf{v}(t-1) + (1 - \beta_2) \cdot \mathbf{g}^2(t)$ ;
     $\hat{\mathbf{m}}(t) = \mathbf{m}(t) / (1 - \beta_1^t)$ ;
     $\hat{\mathbf{v}}(t) = \mathbf{v}(t) / (1 - \beta_2^t)$ ;
     $\mathbf{w}(t) = \mathbf{w}(t-1) - \eta \cdot \hat{\mathbf{m}}(t) / (\sqrt{\hat{\mathbf{v}}(t)} + \epsilon)$ ;
end
return  $\mathbf{w}(t)$ 

```

---

We denote  $\hat{\mathbf{y}}(\mathbf{w}, \mathbf{x})$  as the neural network prediction given the weight vector  $\mathbf{w}$  and input vec-

---

**Algorithm 2:** The extended Kalman Filter (EKF) is an optimizer, where  $\mathbf{A}$  is termed as the scaling matrix,  $\mathbf{K}$  is the Kalman gain,  $\mathbf{P}$  is the error covariance matrix and  $\mathbf{R}$  is the observation-noise covariance matrix. For the sake of discussion, the initial  $\mathbf{P}(0)$  is set to an identity matrix and the process-noise covariance matrix  $\mathbf{Q}$  is set to zero in this work.

---

```

init:  $t = 0$ ,  $\mathbf{P}(0) = \epsilon \mathbf{I}$ ,
while not converged do
     $t = t + 1$ ;
     $\mathbf{J}(t) = \nabla_{\mathbf{w}} \boldsymbol{\xi}(t)$ ;
     $\mathbf{A}(t) = [\mathbf{J}(t) \mathbf{P}(t-1) \mathbf{J}^\top(t) + \mathbf{R}(t)]^{-1}$ ;
     $\mathbf{K}(t) = \mathbf{P}(t-1) \mathbf{J}^\top(t) \mathbf{A}(t)$ ;
     $\mathbf{P}(t) = [\mathbf{I} - \mathbf{K}(t) \mathbf{J}(t)] \mathbf{P}(t-1) + \mathbf{Q}(t)$ ;
     $\mathbf{w}(t) = \mathbf{w}(t-1) + \mathbf{K}(t) \boldsymbol{\xi}(t)$ ;
end
return  $\mathbf{w}(t)$ 

```

---

tor  $\mathbf{x}$ , and  $\mathbf{y}$  as the reference labels.  $\boldsymbol{\xi} = \mathbf{y} - \hat{\mathbf{y}}$  is the error vector. The mean squared error  $L_2 = \frac{1}{n} \sum_i \xi_i^2$  is used as the loss function unless otherwise mentioned.  $\mathbf{g}$  is the gradient of the  $L_2$  loss function with respect to  $\mathbf{w}$ , and  $\mathbf{J}$  is the Jacobian matrix of  $\boldsymbol{\xi}$  with respect to  $\mathbf{w}$ .

The first optimization algorithm used in this work is Adam, which is a popular algorithm for the training of neural networks.<sup>25</sup> The algorithm can be considered as an extension of stochastic gradient descent in which the first moment  $\mathbf{m}(t)$  and second moment  $\mathbf{v}(t)$  are estimated at each step, and used as a preconditioner to the gradients. The algorithm is shown in Algo. 1.

The other optimization algorithm used in this work is EKF, which estimates the internal state of a system given a series of observations over time. In the context of neural network training, it can be interpreted as updating the weights of the neural network according to the gradient of the error with respect to the weights in past samples.<sup>23</sup> The algorithm is summarized in Algo. 2.

## Dataset description

Two datasets containing structures, energies and forces of liquid water (and ice phases) were used to train the NNPs in this work. 6324 structures in the BLYP dataset of both liquid phase and ice phases were taken from Ref. 8 and re-computed with the CP2K suite of programs<sup>28</sup> and the BLYP functional.<sup>29,30</sup> The revPBE0-D3 dataset of 1593 structures of liquid water computed with CP2K was directly taken from Ref. 9.

## Neural Network Potential

In this work, the NNPs were constructed using the BPNN architecture,<sup>6</sup> with the symmetry function taken from Ref. 8. BPNN was implemented previously in the PiNN codebase,<sup>16</sup> which is a TensorFlow-based package for building atomic neural networks for both molecules and materials.<sup>31,32</sup> The default implementation of Adam in TensorFlow was adopted (denoted as PiNN-Adam in the following), and we have implemented the EKF optimizer in TensorFlow (named as PiNN-EKF). To benchmark our EKF implementation, the same dataset was used to train a set of NNPs using the RuNNer code.<sup>19</sup>

The PiNN-Adam models were trained for  $5 \times 10^6$  steps, with a learning rate of  $10^{-4}$  that decays by a factor of 0.994 every  $10^4$  steps. Notably, the gradient clipping technique was used with the Adam optimizer to alleviate the vanishing and exploding gradients problems.<sup>33</sup> The PiNN-EKF models were trained with a learning rate of  $10^{-3}$  for  $5 \times 10^5$  steps. Learning rates were determined with grid search, respectively for each training algorithm. The RuNNer models were trained for 30 epochs, which corresponds to a total of around  $3 \times 10^5$  steps.

In both cases, 80% of the dataset were used for training and the rest 20% were left out as a test set. For each setup, 10 models were trained with different random seeds to split the dataset or initialize the weights of the neural network. Whenever applicable, the standard deviations of the prediction across the models are used as error estimates.

## Molecular Dynamics Simulation

The molecular dynamics (MD) simulations for all the models were carried out with the ASE code in order to make a systematic comparison.<sup>34</sup> The PiNN code supports calculation with ASE, while the RuNNer code<sup>19</sup> was interfaced to ASE through the LAMMPS<sup>35</sup> calculator implemented in ASE. The timestep for all simulations was chosen to be 0.5 fs. The Berendsen barostat and thermostat<sup>36</sup> were used to keep the pressure at 1 bar and temperature at 330 K. The MD simulation was run for 100 ps for each of the trained models.

## Result and discussions

### The extrapolation regime: The case of the BLYP dataset

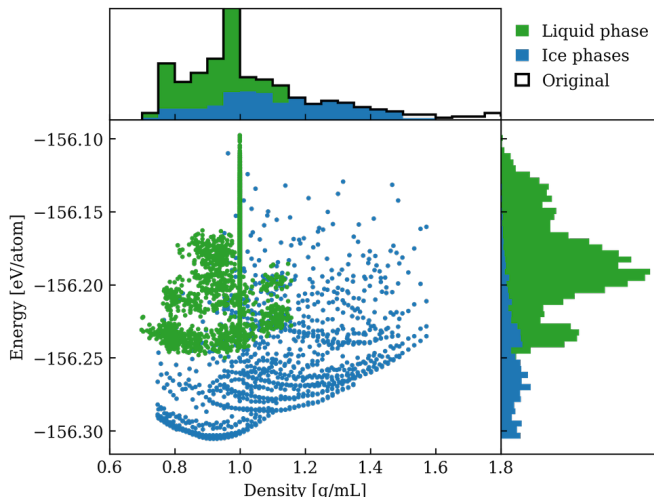


Figure 1: 2D histogram of the BLYP dataset in terms of the total energy per atom and the bulk density.

The energy-density distribution of the BLYP dataset is shown in Fig. 1. This dataset contains structures from both liquid phase and different ice phases with a peak centering at 1.0 g/mL.<sup>8</sup> Given the fact that the equilibrium density of the BLYP water at ambient conditions is below 0.8 g/mL,<sup>8</sup> the isobaric-isothermal density at 1 bar and 330 K will serve as an instructive case study where the NNP is stretched into the extrapolation regime. This

motivates us to discuss the result of the BLYP dataset first, where Adam and EKF show qualitative differences.

Before presenting those results, it is necessary to first discuss the convergence of the NNP trainings. The EKF optimizer is known to converge much faster as compared to Adam (by approximately one order of magnitude in terms of the number of weight updates to achieve the desired accuracy).<sup>20,37</sup> This phenomenon is clear in our training of NNPs, as shown in Fig. 2. However, the actual speed-up is compromised due to the higher computational cost of EKF. In practice, the training takes about 2 h for the EKF optimizer and about 5 h for the Adam optimizer on a 16-core computer to achieve similar levels of accuracy in terms of force and energy. It should be noted that the relative speed advantage per iteration increases drastically when the total number of weights grow.

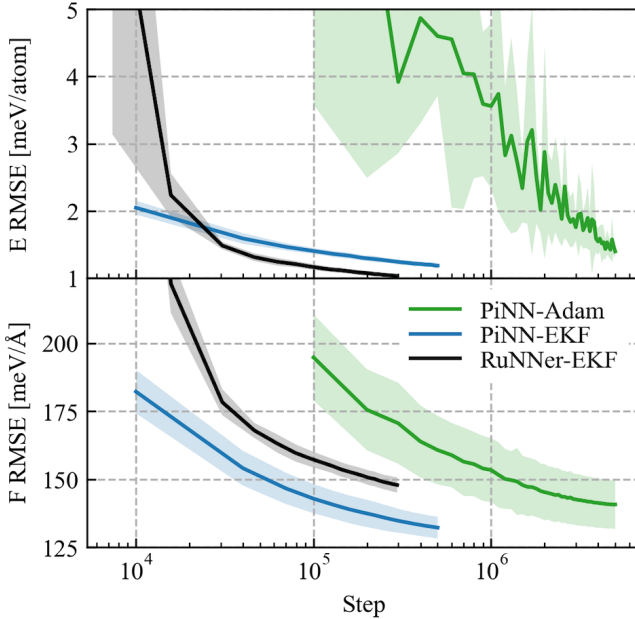


Figure 2: Training curves of the BLYP dataset for a) energy root mean squared error (RMSE) and b) force RMSE with the Adam and the EKF optimizers.

Now we are ready to see how well Adam and EKF estimate the isobaric-isothermal density at ambient conditions for the BLYP dataset. As shown in Fig. 3, at the pressure of 1 bar and the temperature of 330 K, only 2 out of 10 models trained with Adam manage to pre-

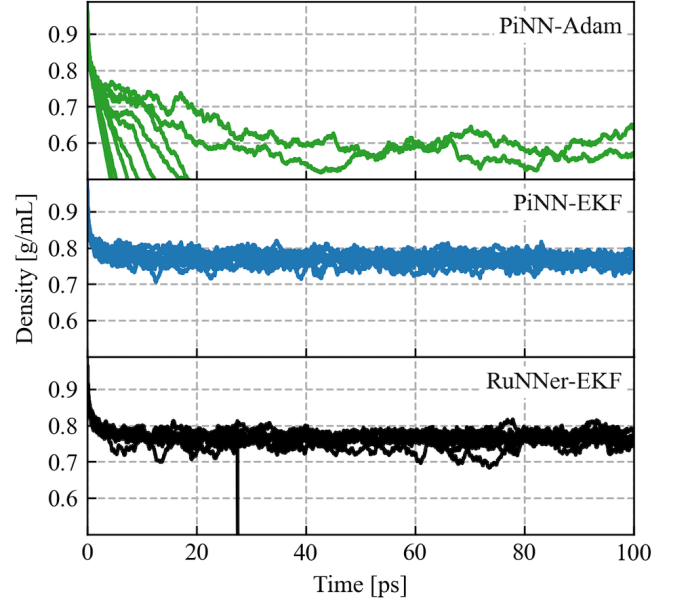


Figure 3: The density ( $\rho$ ) log for NPT simulations using potentials trained with different algorithms.

dict a stable density, while most of the models trained using EKF lead to an excellent agreement with the previously reported density of around 0.76 g/mL for BLYP water.<sup>8</sup> In addition, the EKF implementation in PiNN can reproduce the results of RuNNer well for the same dataset.

The qualitative difference between NNPs trained with Adam and EKF seen in Fig. 3 is striking, in light of comparable force and energy errors shown in Fig. 2. One may argue that the extrapolation is a difficult task for NNPs, because it requires stepping out from their comfort zone. Thus, it is also relevant to consider how the two training algorithms would fare within an interpolation regime. This leads to our second example, the RevPBE0-D3 dataset.

## The interpolation regime: the case of the RevPBE0-D3 dataset

In the following experiment, we have used a dataset that was constructed to cover a wide range in the configuration space uniformly,<sup>9</sup> as seen in the energy-density distribution in Fig. 4.

With this dataset, both Adam and EKF yield physical densities at the given temperature.

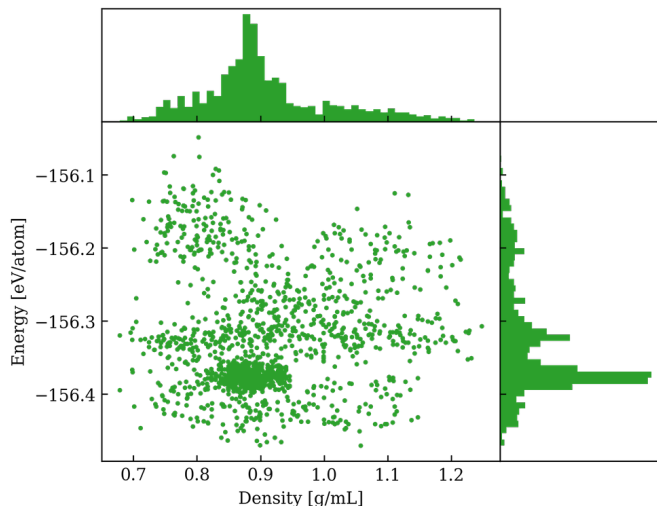


Figure 4: 2D histogram of the RevPBE0-D3 dataset in terms of the total energy per atom and the bulk density.

However, as shown in Fig. 5, the density prediction strongly depends on the learning rate used to train the model in the case of Adam.

It is tempting to conclude that the models trained with larger learning rates are the better performing ones due to smaller force and energy errors. Similarly to the observation made for the BLYP dataset, the error metrics do not seem to correspond to the actual prediction performance of the trained NNPs. Indeed, we notice that the density does not seem to converge when the error metrics (Fig. 5) have reached lower values. Given that the reference density value for this dataset at 1 bar and 320 K is 0.92 g/ml,<sup>9</sup> this suggests that one has to re-think the common wisdom on performing model selection based on error metrics.

Regardless of this implication, the present case study demonstrates that the performance of NNPs can be sensitive to the learning rate, in particular for Adam. As a consequence, this can lead to a tangible difference in terms of the density prediction even within the interpolation regime where the dataset already has a good coverage.

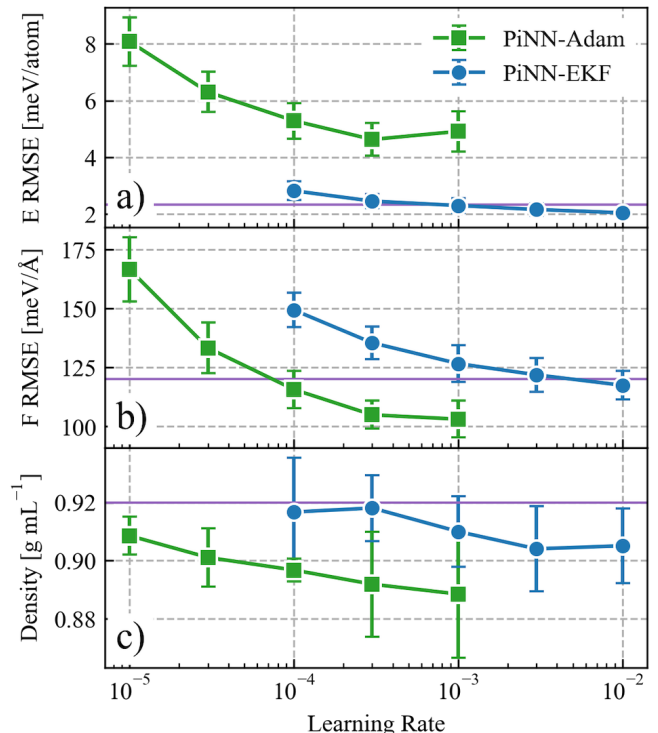


Figure 5: RMSE and density predictions for NNPs trained with different algorithms: a) energy RMSE; b) force RMSE and c) density predictions at 320K, 1bar. Reference values from ref. 9 is shown in purple.

## Differences in models trained using Adam and EKF

In the previous sections, we found that NNPs trained with EKF seem to be less sensitive to the learning rate and more generalizable. Meanwhile, it is also clear that model selection based on the error metrics of energy and force may not always lead to a sound choice. Then, the questions are i) can we distinguish “good” and “bad” NNPs by just looking into the weight space (rather than doing the actual MD simulations for the density prediction)? ii) why does EKF do better for training NNPs than Adam?

To answer the first question, we have analyzed the models presented in the earlier sections to shed some light on the characteristics of the models trained with Adam and EKF.

One common measure to distinguish different models is the Euclidean distance of the optimized weights to those in the initialization.<sup>38</sup> Denoting the vector of all weight variables in

the neural network as  $\mathbf{w}$ , we also compared the evolution of the weights distance from initialization  $\|\Delta\mathbf{w}\| = \|\mathbf{w} - \mathbf{w}_{\text{init}}\|$ , and the distribution of the weights  $w_i$  of the final models for the trained networks.

As shown in Fig 6a, different NNPs trained on the BLYP dataset display similar weights distances from initialization. Moreover, the weight distributions of NNPs trained with Adam and EKF are almost indistinguishable as shown in Fig. 6b. This suggests that the norm-based measure also fails to distinguish models obtained from Adam and EKF. It further hints that using a  $L_2$  norm-based regularization may not improve the performance of NNPs.

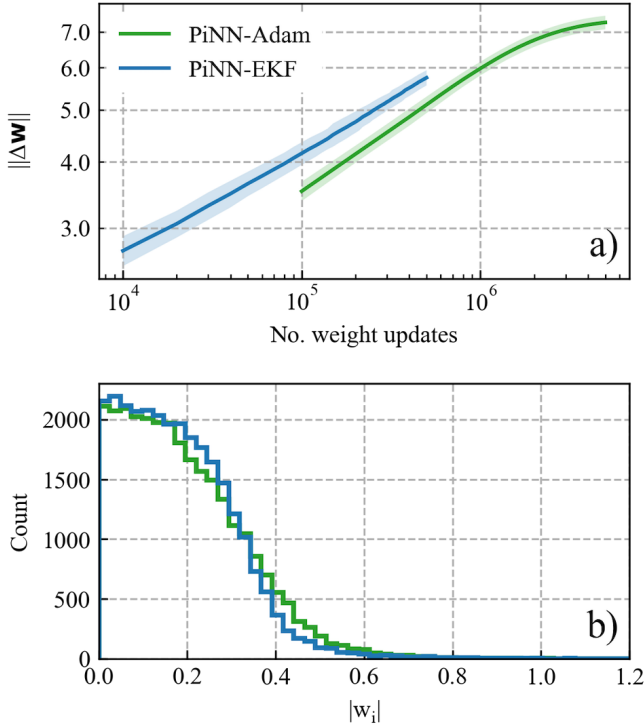


Figure 6: Weight-based measures for NNPs trained with Adam and EKF for the BLYP dataset: a) the evolution of the Euclidean weight distance from initialization  $\|\Delta\mathbf{w}\|$  and b) the distribution of weights  $w_i$ .

Another class of similarity measure is related to the local information geometry of the neural network.<sup>39</sup> Here, we characterized it with the Fisher information matrix  $\mathcal{I}$ .

$$\langle \mathcal{I}_1 \rangle_t = \langle (\nabla_{\mathbf{w}} L_1(\boldsymbol{\xi}(t)))^{\otimes 2} \rangle \quad (1)$$

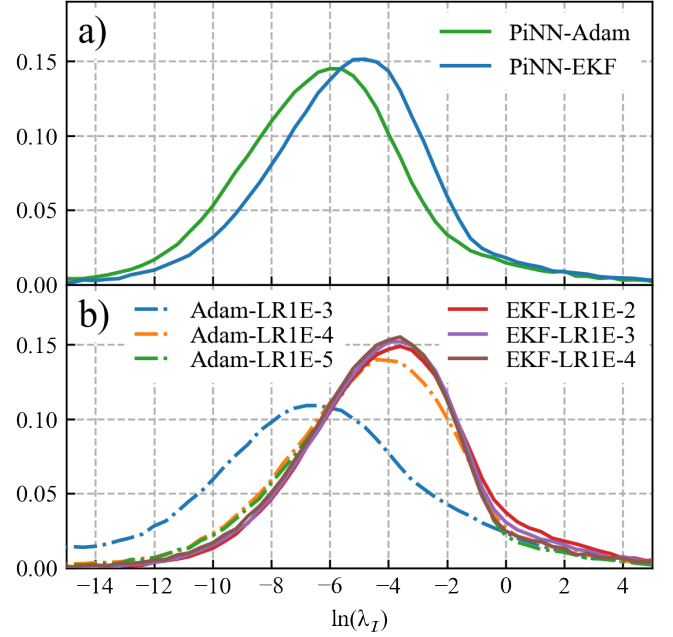


Figure 7: Distributions of the eigenvalues ( $\lambda_I$ ) of the Fisher information matrix: a) with different training algorithms for the BLYP dataset; b) with different training algorithm and learning rates for the revPBE0-D3 dataset.

Here we used  $L_1$  loss instead of  $L_2$  loss to construct the Fisher information matrix for reasons that will be clear later. Fig. 7 shows the distribution of eigenvalues  $\lambda_I$  of the Fisher information. For the BLYP dataset, EKF found local minima with much larger eigenvalues as compared to Adam, where the peak of the distribution differs by about one order of magnitude (note the logarithm scale used here). Therefore, the Fisher information is a similarity measure which can effectively distinguish the performance of NNPs.

A similar trend was observed for the revPBE0-D3 dataset. The eigenvalue distribution of NNP trained with Adam and a small learning rate (1E-5) is more close to those trained with EKF. This deviation becomes larger when increasing the learning rate (1E-4 and 1E-3). In contrast, eigenvalue distributions of NNPs trained with EKF are almost identical. These results correlate well with the density prediction from MD simulations as shown in Fig. 5.

The usefulness of the Fisher information for

model selection is also linked to the second question posed at the beginning of this section. Despite different motivations, both Adam and EKF can be understood in terms of natural gradient descent (NGD), where the inverse of the Fisher information matrix  $\mathcal{I}$  is used as a preconditioner.

In Adam,  $\mathcal{I}$  is approximated as a diagonal matrix, with the diagonal terms thereof being the second moment vector  $\hat{\mathbf{v}}(t)$ . The inverse square root of the diagonal elements are used as a conservative preconditioner.

On the other hand, the connection between EKF and NGD has been shown recently,<sup>40</sup> where the inverse  $\mathcal{I}$  matrix is effectively estimated by the error covariance matrix  $\mathbf{P}$  in EKF. In fact, one can show that

$$\mathbf{w}(t) = \mathbf{w}(t-1) - \frac{\eta^2}{2t} \langle \mathcal{I}_1 \rangle_t^{-1} \mathbf{g}(t) \quad (2)$$

where the covariance matrix of observation noise  $\mathbf{R}$  in Algo. 2 is chosen to be a scaled identity matrix,<sup>20,37</sup> i.e.  $\mathbf{R}(t) = \frac{1}{\eta} \mathbf{I}$ .

This means EKF can be viewed as the on-line estimate of the full Fisher information  $\mathcal{I}$  with respect to  $L_1$  loss and the  $1/t$  decay of the learning rate. We think such feature leads to a good similarity measure of models using the Fisher information based on Eq. 1 and a superior performance of EKF for training NNPs as demonstrated in two case studies shown in this work.

## Conclusion and outlook

To sum up, we have compared the performance of two optimization algorithms Adam and EKF for training NNPs of liquid water based on BLYP and revPBE0-D3 datasets. It is found that NNPs trained with EKF are more transferable and less sensitive to the choice of the learning rate, as compared to Adam. Further, we show that the Fisher information is a useful similarity measure for the model selection of NNPs when the error metrics and the normal-based measure become ineffective.

Established practice in other neural network applications,<sup>41</sup> using Adam, indicate that prac-

tical training performance can be improved if an architecture is reparametrized to promote weights in a common numerical range, without strong correlations. Another future avenue would thus be to preserve the expressive power of existing NNPs, while expressing the weights in such a way that the off-diagonal elements of the resulting Fisher information matrix are minimized. This can be understood in terms of the limitations in the Adam preconditioner strategy.

Before closing, it is worth to note that the present issue of training algorithms may be overcome with more data, for which a number of active-learning approaches have been proposed.<sup>11,42</sup> However, we would argue that a better training algorithm does not only improve the performance of NNPs but also improve the data efficiency in the active-learning. Finally, we are aware of the so-called “no free lunch theorem”<sup>43</sup> when it comes to the optimization, therefore our conclusions regarding the comparison of Adam and EKF are limited to training NNPs and this calls for more comparative studies to shed light on this topic.

**Acknowledgement** CZ thanks the Swedish Research Council (VR) for a starting grant (No. 2019-05012). We also acknowledge the Swedish National Strategic e-Science program eSSSENCE for funding. Part of the simulations were performed on the resources provided by the Swedish National Infrastructure for Computing (SNIC) at UPPMAX and NSC.

## References

- (1) Behler, J. Four Generations of High-Dimensional Neural Network Potentials. *Chem. Rev.* **2021**, DOI: 10.1021/acs.chemrev.0c00868.
- (2) Deringer, V. L.; Bartók, A. P.; Bernstein, N.; Wilkins, D. M.; Ceriotti, M.; Csányi, G. Gaussian Process Regression for Materials and Molecules. *Chem. Rev.* **2021**, DOI: 10.1021/acs.chemrev.1c00022.
- (3) Watanabe, S.; Li, W.; Jeong, W.; Lee, D.;

- Shimizu, K.; Mimanitani, E.; Ando, Y.; Han, S. High-dimensional neural network atomic potentials for examining energy materials: some recent simulations. *J. Phys.: Energy* **2020**, *3*, 012003.
- (4) Unke, O. T.; Chmiela, S.; Sauceda, H. E.; Gastegger, M.; Poltavsky, I.; Schütt, K. T.; Tkatchenko, A.; Müller, K.-R. Machine Learning Force Fields. *Chem. Rev.* **2021**, *121*, 10142–10186.
- (5) Jia, W.; Wang, H.; Chen, M.; Lu, D.; Lin, L.; Car, R.; Weinan, E.; Zhang, L. Pushing the Limit of Molecular Dynamics with Ab Initio Accuracy to 100 Million Atoms with Machine Learning. SC20: International Conference for High Performance Computing, Networking, Storage and Analysis. 2020; pp 1–14.
- (6) Behler, J.; Parrinello, M. Generalized Neural-Network Representation of High-Dimensional Potential-Energy Surfaces. *Phys. Rev. Lett.* **2007**, *98*.
- (7) Gastegger, M.; Behler, J.; Marquetand, P. Machine learning molecular dynamics for the simulation of infrared spectra. *Chem. Sci.* **2017**, *8*, 6924–6935.
- (8) Morawietz, T.; Singraber, A.; Dellago, C.; Behler, J. How van der Waals interactions determine the unique properties of water. *Proc. Natl. Acad. Sci. U.S.A* **2016**, *113*, 8368–8373.
- (9) Cheng, B.; Engel, E. A.; Behler, J.; Dellago, C.; Ceriotti, M. Ab initio thermodynamics of liquid and solid water. *Proc. Natl. Acad. Sci.* **2019**, *116*, 1110–1115.
- (10) Quaranta, V.; Hellström, M.; Behler, J. Proton-Transfer Mechanisms at the Water-ZnO Interface: The Role of Pre-solvation. *J. Phys. Chem. Lett.* **2017**, *8*, 1476–1483.
- (11) Schran, C.; Behler, J.; Marx, D. Automated Fitting of Neural Network Potentials at Coupled Cluster Accuracy: Protonated Water Clusters as Testing Ground. *J. Chem. Theory Comput.* **2019**, *16*, 88–99.
- (12) Shao, Y.; Hellström, M.; Yllö, A.; Mindemark, J.; Hermansson, K.; Behler, J.; Zhang, C. Temperature effects on the ionic conductivity in concentrated alkaline electrolyte solutions. *Phys. Chem. Chem. Phys.* **2020**, *377*, 1–5.
- (13) Lecun, Y.; Bengio, Y.; Hinton, G. Deep learning. *Nature* **2015**, *521*, 436–444.
- (14) Schütt, K. T.; Sauceda, H. E.; Kindermans, P.-J.; Tkatchenko, A.; Müller, K.-R. SchNet A deep learning architecture for molecules and materials. *J. Chem. Phys.* **2018**, *148*, 241722.
- (15) Chen, C.; Ye, W.; Zuo, Y.; Zheng, C.; Ong, S. P. Graph Networks as a Universal Machine Learning Framework for Molecules and Crystals. *Chem. Mater.* **2019**, *31*, 3564–3572.
- (16) Shao, Y.; Hellström, M.; Mitev, P. D.; Knijff, L.; Zhang, C. PiNN: A Python Library for Building Atomic Neural Networks of Molecules and Materials. *J. Chem. Inf. Model.* **2020**, *60*, 1184–1193.
- (17) Gastegger, M.; Marquetand, P. High-Dimensional Neural Network Potentials for Organic Reactions and an Improved Training Algorithm. *J. Chem. Theory Comput.* **2015**, *11*, 2187–2198.
- (18) Artrith, N.; Urban, A. An implementation of artificial neural-network potentials for atomistic materials simulations: Performance for TiO<sub>2</sub>. *Comput. Mater. Sci.* **2016**, *114*, 135–150.
- (19) Behler, J. RuNNet-A Neural Network Code for High-Dimensional Potential-Energy Surfaces. 2018.
- (20) Singraber, A.; Morawietz, T.; Behler, J.; Dellago, C. Parallel Multistream Training of High-Dimensional Neural Network Potentials. *J. Chem. Theory Comput.* **2019**, *15*, 3075–3092.

- (21) Huang, S.-D.; Shang, C.; Kang, P.-L.; Zhang, X.-J.; Liu, Z.-P. LASP: Fast global potential energy surface exploration. *WIREs Comput. Mol. Sci.* **2019**, *9*, e1415–11.
- (22) Liu, D. C.; Nocedal, J. On the limited memory BFGS method for large scale optimization. *Math. Program.* **1989**, *45*, 503–528.
- (23) Singhal, S.; Wu, L. Training Multilayer Perceptrons with the Extended Kalman Algorithm. Proceedings of the 1st International Conference on Neural Information Processing Systems. Cambridge, MA, USA, 1988; p 133–140.
- (24) Gao, X.; Ramezanghorbani, F.; Isayev, O.; Smith, J. S.; Roitberg, A. E. TorchANI: A Free and Open Source PyTorch-Based Deep Learning Implementation of the ANI Neural Network Potentials. *J. Chem. Inf. and Model.* **2020**, *60*, 3408–3415, PMID: 32568524.
- (25) Kingma, D. P.; Ba, J. Adam: A Method for Stochastic Optimization. *arXiv 1412.6980v9* **2014**, 1–15.
- (26) Abadi, M.; Agarwal, A.; Barham, P.; Brevdo, E.; Chen, Z.; Citro, C.; Corrado, G. S.; Davis, A.; Dean, J.; Devin, M.; Ghemawat, S.; Goodfellow, I.; Harp, A.; Irving, G.; Isard, M.; Jia, Y.; Jozefowicz, R.; Kaiser, L.; Kudlur, M.; Levenberg, J.; Mané, D.; Monga, R.; Moore, S.; Murray, D.; Olah, C.; Schuster, M.; Shlens, J.; Steiner, B.; Sutskever, I.; Talwar, K.; Tucker, P.; Vanhoucke, V.; Vasudevan, V.; Viégas, F.; Vinyals, O.; Warden, P.; Wattenberg, M.; Wicke, M.; Yu, Y.; Zheng, X. TensorFlow: Large-Scale Machine Learning on Heterogeneous Systems. 2015; <https://www.tensorflow.org/>, Software available from tensorflow.org.
- (27) Paszke, A.; Gross, S.; Massa, F.; Lerer, A.; Bradbury, J.; Chanan, G.; Killeen, T.; Lin, Z.; Gimelshein, N.; Antiga, L.; Desmaison, A.; Kopf, A.; Yang, E.; DeVito, Z.; Raison, M.; Tejani, A.; Chilamkurthy, S.; Steiner, B.; Fang, L.; Bai, J.; Chintala, S. In *Advances in Neural Information Processing Systems 32*; Wallach, H., Larochelle, H., Beygelzimer, A., d’Alché Buc, F., Fox, E., Garnett, R., Eds.; Curran Associates, Inc., 2019; pp 8024–8035.
- (28) Kühne, T. D.; Iannuzzi, M.; Ben, M. D.; Rybkin, V. V.; Seewald, P.; Stein, F.; Laino, T.; Khaliullin, R. Z.; Schütt, O.; Schiffmann, F.; Golze, D.; Wilhelm, J.; Chulkov, S.; Bani-Hashemian, M. H.; Weber, V.; Borštnik, U.; Taillefumier, M.; Jakobovits, A. S.; Lazzaro, A.; Pabst, H.; Müller, T.; Schade, R.; Guidon, M.; Andermatt, S.; Holmberg, N.; Schenter, G. K.; Hehn, A.; Bussy, A.; Belleflamme, F.; Tabacchi, G.; Glöß, A.; Lass, M.; Bethune, I.; Mundy, C. J.; Plessl, C.; Watkins, M.; VandeVondele, J.; Krack, M.; Hutter, J. CP2K: An electronic structure and molecular dynamics software package - Quickstep: Efficient and accurate electronic structure calculations. *J. Chem. Phys.* **2020**, *152*, 194103.
- (29) Becke, A. D. Density-functional exchange-energy approximation with correct asymptotic behavior. *Phys. Rev. A* **1988**, *38*, 3098.
- (30) Lee, C.; Yang, W.; Parr, R. G. Development of the Colle-Salvetti correlation-energy formula into a functional of the electron density. *Phys. Rev. B* **1988**, *37*, 785.
- (31) Shao, Y.; Knijff, L.; Dietrich, F. M.; Hermansson, K.; Zhang, C. Modelling Bulk Electrolytes and Electrolyte Interfaces with Atomistic Machine Learning. *Batter. Supercaps* **2021**, *4*, 585–595.
- (32) Knijff, L.; Zhang, C. Machine learning inference of molecular dipole moment in liquid water. *Mach. Learn.: Sci. Technol.* **2021**, *2*, 03LT03.

- (33) Pascanu, R.; Mikolov, T.; Bengio, Y. On the difficulty of training recurrent neural networks. *Proceedings of the 30th International Conference on Machine Learning*. Atlanta, Georgia, USA, 2013; pp 1310–1318.
- (34) Larsen, A. H.; Mortensen, J. J.; Blomqvist, J.; Castelli, I. E.; Christensen, R.; Dulak, M.; Friis, J.; Groves, M. N.; Hammer, B.; Hargus, C.; Hermes, E. D.; Jennings, P. C.; Jensen, P. B.; Kermode, J.; Kitchin, J. R.; Kolsbjerg, E. L.; Kubal, J.; Kaasbjerg, K.; Lysgaard, S.; Maronsson, J. B.; Maxson, T.; Olsen, T.; Pastewka, L.; Peterson, A.; Rostgaard, C.; Schiøtz, J.; Schütt, O.; Strange, M.; Thygesen, K. S.; Vegge, T.; Vilhelmsen, L.; Walter, M.; Zeng, Z.; Jacobsen, K. W. The atomic simulation environment—a Python library for working with atoms. *J. Phys.: Condens. Matter* **2017**, *29*, 273002.
- (35) Plimpton, S. Fast Parallel Algorithms for Short-Range Molecular Dynamics. *J. Comput. Phys.* **1995**, *117*, 1–19.
- (36) Berendsen, H. J. C.; Postma, J. P. M.; van Gunsteren, W. F.; DiNola, A.; Haak, J. R. Molecular dynamics with coupling to an external bath. *J. Chem. Phys.* **1984**, *81*, 3684–3690.
- (37) Ruck, D.; Rogers, S.; Kabrisky, M.; Maybeck, P.; Oxley, M. Comparative analysis of backpropagation and the extended Kalman filter for training multilayer perceptrons. *IEEE Transactions on Pattern Analysis and Machine Intelligence* **1992**, *14*, 686–691.
- (38) Nagarajan, V.; Kolter, J. Z. Generalization in Deep Networks: The Role of Distance from Initialization. *arXiv 1901.01672v2* **2019**, 1–15.
- (39) Liang, T.; Poggio, T.; Rakhlin, A.; Stokes, J. Fisher-Rao Metric, Geometry, and Complexity of Neural Networks.
- (40) Ollivier, Y. Online Natural Gradient as a Kalman Filter. *arXiv 1703.00209v3* **2018**, 1–34.
- (41) Ioffe, S.; Szegedy, C. Batch Normalization: Accelerating Deep Network Training by Reducing Internal Covariate Shift. *Proceedings of the 32nd International Conference on Machine Learning*. Lille, France, 2015; pp 448–456.
- (42) Zhang, Y.; Wang, H.; Chen, W.; Zeng, J.; Zhang, L.; Wang, H.; E, W. DP-GEN: A concurrent learning platform for the generation of reliable deep learning based potential energy models. *Comput. Phys. Commun.* **2020**, *253*, 107206.
- (43) Wolpert, D.; Macready, W. No free lunch theorems for optimization. *IEEE Transactions on Evolutionary Computation* **1997**, *1*, 67–82.

## Graphical TOC Entry

